

Fabrication of a Dual-axis Auto Solar Tracking System

Ho-Sheng Chen,¹ Xiao-Qing Lin,² Chao-Ming Hsu,^{2*} and Cheng-Fu Yang^{3,4**}

¹School of Technology, Fuzhou Technology and Business University, Fuzhou, Fujian 350715, China

²Department of Mechanical Engineering, National Kaohsiung University of Science and Technology,
Kaohsiung 807, Taiwan

³Department of Chemical and Materials Engineering, National University of Kaohsiung,
Kaohsiung 811, Taiwan

⁴Department of Aeronautical Engineering, Chaoyang University of Technology,
Taichung 413, Taiwan

(Received March 31, 2025; accepted May 26, 2025)

Keywords: cost-effective and dual-axis solar tracking mechanism, SolidWorks CAD software, finite element analysis software

A complete solar tracking system consists of several key components: a concentrator, a receiver, and the electromechanical equipment that together convert sunlight into electrical energy. In addition, a tracking structure is necessary to allow solar panels to follow the sun's path, maximizing the amount of sunlight they can capture throughout the day. This structure must also incorporate sensor elements that precisely track the sun's position to ensure optimal performance. Lastly, a control system is needed to efficiently manage and utilize the collected energy. In this research, we focused on reducing manufacturing costs and increasing solar power output while ensuring the system's safety and stability. The goal was to provide a straightforward method for constructing the system, using both functional and strength design principles to create a simple yet effective dual-axis auto solar tracking mechanism. The development process began with designing the tracking mechanism using AutoCAD to generate detailed engineering drawings that specified dimensions and tolerances. A bill of materials was also created, and an initial cost was estimated. The manufacturing of the mechanism was then outsourced to the most suitable supplier. Before assembly, a series of functionality tests were conducted, followed by continuous revisions and adjustments. These iterative tests ensured the mechanism's safety and performance. Once the system met all the design requirements outlined in this research, the production process was considered complete.

1. Introduction

The dual-axis solar tracking system is an advanced and highly efficient solar tracking technology designed to maximize the amount of sunlight absorbed by solar panels, thereby increasing energy production.⁽¹⁾ Unlike traditional fixed or single-axis tracking systems, the dual-axis system can track the sun's movement in two directions. This allows it to precisely align with the sun in accordance with the day and year, ensuring optimal solar exposure at all times.

*Corresponding author: e-mail: jammy@nkust.edu.tw

**Corresponding author: e-mail: cfyang@nuk.edu.tw

<https://doi.org/10.18494/SAM5671>

The system consists of several key components that work together to achieve this high level of efficiency. The dual-axis tracking structure includes an azimuth axis, which enables the solar panels to rotate horizontally, adjusting to the sun's east-to-west movement. The elevation axis allows the panels to tilt vertically, compensating for changes in the sun's height during the day. This dual movement ensures the panels are always positioned to capture the maximum amount of sunlight. Sensors or light detectors are used to precisely track the sun's location.⁽²⁾ These sensors monitor the intensity of solar radiation and adjust the angle of the solar panels accordingly to ensure they are always facing the sun. The control system processes the data from the sensors and sends commands to adjust the panel's angle, keeping the system continuously aligned with the sun.

This dynamic adjustment improves the light reception efficiency and boosts power generation. Servo motors are typically employed to rotate the two axes, responding to the control system's commands to adjust the panels' positions. The main advantage of the dual-axis tracking system is its ability to precisely follow the sun's path, capturing more sunlight than a fixed or single-axis system. This results in a significant increase in energy output.⁽³⁾ The system adapts to the sun's position in accordance with the day and the year, ensuring maximum sunlight capture regardless of the season or time of day. Additionally, it can be deployed in various geographical locations and climates, delivering consistent performance whether near the equator or close to the poles. In conclusion, the dual-axis solar tracking system is an extremely effective solution for maximizing solar energy capture. Although more complex and costly than traditional systems, its ability to significantly boost energy production makes it an ideal choice for applications that demand high efficiency. The dual-axis solar tracking system has been under development for many years. Building upon this concept, Roth and his team developed a dual-axis solar tracking platform using a quadrant sensor to automatically measure solar radiation.⁽⁴⁾ Under overcast conditions, their system used a computational procedure to estimate the sun's position, employing movement control to adjust the platform until the sensor could once again detect sunlight.⁽⁴⁾ Their investigated system could automatically measure direct solar radiation using a pyrheliometer and operated autonomously, guided by a closed-loop servo system.

Batayneh *et al.* designed a fuzzy logic controller for a dual-axis solar tracking photovoltaic (PV) system.⁽⁵⁾ The system has a 50 W PV panel, and the tracking structure is of the single-column type. The system employs two DC motors and utilized photovoltaic sensors mounted on all four sides of the solar panel to calculate the corresponding output signals, which then drives the motors to adjust the position of the solar panel.⁽⁵⁾ Shaw *et al.* focused on controlling a dual-axis solar tracking system, with the primary goal of maximizing the power efficiency of the photovoltaic module by adjusting its angle to maintain a perpendicular alignment between the sun and the PV module.⁽⁶⁾ Their system incorporated two motors and various electronic sensors placed at different positions to facilitate precise adjustments of the PV module.⁽⁶⁾ This system relied on the integration of a linear Fresnel concentrator with a channel photovoltaic/thermal collector. In 2021, Aji *et al.* proposed the design and simulation of a dual-axis solar tracker, allowing the solar module to easily move along two axes of rotation to track the sun's movement from east to west and north to south, optimizing solar energy generation.⁽⁷⁾ The tracking system is designed as an adaptive system based on closed-loop monitoring, utilizing light-dependent

resistor (LDR) sensors for device input, servo motors for module adjustments, and an Arduino Uno as the system's controller.⁽⁷⁾

In this study, we referenced previous literature and approached the design from the perspective of functionality. We compared the effects of different types of solar tracking system on efficiency, as well as the regional adaptability of these tracking methods, and then selected a direction to proceed with the next design steps. After determining the design objectives, the conceptual design was divided into evaluations of the solar panel truss, structural form, and drive mechanism. Next, the detailed design of the mechanism was carried out, starting with the selection of the bearing size and model, the number and positions of screws, and the welding conditions at the joints. To reduce manufacturing costs, the mechanical design catalog was first consulted to find the most suitable standard components, with all parts listed in detail. The components were then purchased on the basis of their type. If other similarly sized and compatible parts were available, their 3D models were adjusted accordingly, and assembly drawings were created once all component models, dimensions, and installation positions were confirmed. If there was any interference, the design was revised; if there was no interference, the design was analyzed using finite element analysis software to check whether the structural strength met the safety standards. If the strength did not meet the required standards, the conceptual design was revisited and adjustments were made to the weak structures. If the strength met the standards, the solar tracking mechanism design was considered complete.

2. Design and Fabrication Processes

First, we had to consider the arrangement of the four solar panels to be mounted on the mechanism. The dimensions of a single solar panel were 1.639 m by 0.983 m. Owing to spatial constraints at the installation site, the azimuth rotation diameter was only 4 m. By aligning two panels together, forming a 2×2 arrangement, the total area of the panels measured 3.264 m in length and 1.966 m in width, with the azimuth rotation diameter reduced to 3.822 m. Next, the operational method of the four solar panels was considered. If a linkage mechanism were used to rotate the panels individually, a large amount of space would be required. If the panels were placed too closely, the shadows generated during rotation could impact the power generation of the other panels. Therefore, we decided to create a large truss structure that allowed all four panels to rotate together, and then the direction of panel rotation was then determined. If the long edge was used as the tilt axis, the required rotation radius for the tilt angle would be 0.983 m. However, if the short edge was used as the tilt axis, the required rotation radius for the tilt angle would be 1.639 m. Given the spatial limitations, we chose to use the short edge as the tilt axis for the panels. Owing to the initial design of the support structure, there was a problem of difficulty in calibrating the level during assembly. Therefore, the azimuth rotation structure was changed to a single-column structure. This modification is shown in Fig. 1(a). Considering ease of disassembly, the entire structure was constructed using aluminum extrusions.

Additionally, the space required for the installation of the electronic control system was found to be smaller than initially anticipated. As a result, the azimuth rotation mechanism was directly connected to the tilt mechanism, and the final design is shown in Fig. 1(b). Solar tracking systems are classified into three types on the basis of their control mechanisms: active,

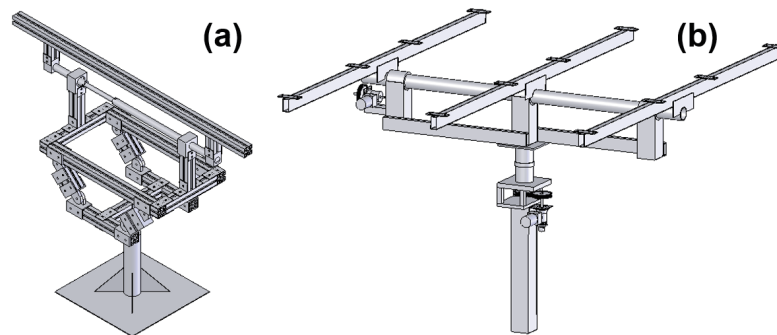


Fig. 1. (Color online) (a) Concept diagram of modified design and (b) concept diagram of final design.

passive, and hybrid. Active tracking systems use light sensors to detect the sun's position and adjust the tracking angle on the basis of user-defined detection frequency, making them a closed-loop system. In contrast, passive tracking systems, also called open-loop systems, calculate the actuator's movement on the basis of solar trajectories and the installation site's latitude and longitude, determining the annual movement path. The tracking angle can be calculated in several ways: one method uses celestial coordinate systems (e.g., ecliptic, equatorial, or horizontal coordinates), and another calculates the solar zenith angle, elevation, and azimuth by considering solar time and its relationship with the equator. We tracked the sun using the elevation and azimuth angles. The axis design consisted of one axis parallel to the ground and another perpendicular to it. Owing to space limitations, the mechanism was placed below the solar panel, and the elevation axis was also positioned below the panel. As the tracking mechanism moved, there were angular limitations, as shown in Fig. 1(a). To address radial space restrictions around the elevation axis, the support structure was divided into two parts. The upper part used two square tubes to connect to the solar panel's frame, whereas the lower part used four round tubes for added strength. The control system was housed within the support frame, and a rotating disc linked to the frame was designed to drive the elevation mechanism.

Figure 2(a) shows the assembly diagram of the elevation angle rotation mechanism, whereas Fig. 2(b) provides an enlarged view of the elevation angle transmission mechanism. The mechanism was divided into different components on the basis of its assembly, including the structure for fixing the solar panel, the elevation rotation shaft, the passive gear shaft, the main beam of the elevation structure, and the fixed mount for the elevation motor. Since the transmission components used spur gears, the rotation axis of the elevation rotation shaft had to be aligned with the rotation axis of the passive gear in the transmission mechanism. To facilitate assembly, the two shafts were first welded individually using flanges at their ends, and then the shafts were connected through the flange. Both ends of the elevation rotation shaft were fitted with ball bearings to reduce friction during the mechanism's rotation. To prevent axial displacement of the rotation shaft, stepped sections were machined at both ends of the shaft. For the stepped sections to be properly machined on a round tube, the tube wall thickness had to be sufficient, so an SCH40 grade tube was chosen. Finally, the bearings were inserted into the rotating shaft and fixed onto the H-shaped steel. For the design of the elevation transmission mechanism, the passive gear shaft and the fixed mount for the elevation motor were separated.

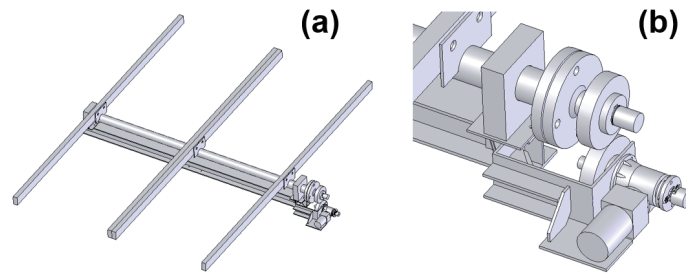


Fig. 2. (Color online) (a) Assembly diagram of elevation angle rotation mechanism and (b) enlarged view of elevation angle transmission mechanism.

To limit axial displacement of the gear on the passive shaft, a stepped section was machined at the left end of the shaft, and a retaining ring was placed at the right end. The fixed mount for the elevation motor was made by welding four 6-mm-thick steel plates together. The dual-axis solar tracking mechanism designed in this study was evaluated using the simulation of the finite element analysis software MSC.Marc. The system was capable of dual-axis operation, could support solar panels weighing up to 80 kg, withstand typhoon winds of up to level 17, and was resistant to earthquakes up to magnitude 5. The solar tracking system developed in this study was primarily constructed using commercially available standard components. This approach minimizes the need for custom-fabricated parts, thereby significantly reducing production costs. As a result, the total system cost was effectively controlled within a budget of NT\$80000, demonstrating the feasibility of implementing a cost-efficient yet functional solar tracking solution. The solar tracking system developed in this study is priced significantly lower than comparable commercial systems—at less than one-fifth of the cost of typical market-available solutions. This substantial reduction in cost highlights the system's potential for scalable application in budget-conscious or resource-limited environments, without compromising core functionality.

In this study, an altitude-azimuth dual-axis solar tracking system was adopted. The rotation axes were designed such that one is parallel to the azimuth axis and the other is perpendicular to the elevation axis. To address spatial constraints, the tracking mechanism was installed beneath the solar panel. Azimuthal rotation was achieved using a circular support frame integrated with a circular rail, while the elevation axis was positioned below the solar panel, although its movement was subject to angular limitations owing to spatial constraints. To accommodate the radial space limitations centered around the elevation rotation mechanism, the support structure was divided into upper and lower segments. To meet the required elevation tracking angles, the upper support structure employed two rectangular tubes to connect with the truss structure of the solar panel. For enhanced structural rigidity, the lower support frame used four circular tubes for connection. The control system was housed within the inner space of the support structure. Additionally, a rotary disk, mechanically linked to the rotation mechanism, was integrated within the rotating frame. This rotary disk was elevated to drive the elevation tracking mechanism effectively.

3. Results and Discussion

In this study, we focused on static structural analysis. The thermal expansion generated within the temperature range of 20 to 40 °C does not affect the operation of the mechanism. Therefore, the material properties only need to be set on the basis of the density, Poisson's ratio, and Young's modulus at room temperature. The selected materials are shown in Fig. 3(a). The four upper pipes of the mechanism are made of 6061 aluminum, whereas the remaining components are made of A36 steel. After the assembly of the mechanism, the base plate was fixed to the concrete foundation using hexagonal nuts and bolts, ensuring no vertical displacement between the bottom surface of the base plate and the ground. The bolt holes on the base plate will not have any lateral displacement. The boundary conditions were set as shown in Fig. 3(b); boundary condition 1 shows that the displacement in the z-direction of the bottom surface of the base plate is zero. In Fig. 3(c), boundary condition 2 shows that there is no displacement in the xy-plane at the contact surface between the base plate holes and the foundation bolts.

After completing the engineering drawings, the next step was to begin the fabrication of the mechanism. First, materials were prepared to facilitate the subsequent assembly process. After the plate material had been processed, it was crucial to verify the accuracy of the component dimensions before initiating the welding process. The components were first arranged and assembled for preliminary checks, and once all materials were confirmed to be correct, welding lines were drawn, and the welding process was begun. In this study, the bearing housings for both the elevation rotation mechanism and the azimuth rotation mechanism were processed and welded by identical methods. This involved drilling holes for the bearings into iron blocks, followed by welding the iron blocks to the plates. Once all components were fabricated, a pre-assembly was conducted in the factory to ensure that no interference occurred during operation. This was a critical step, as any interference could lead to performance issues or even damage during actual use. Once all component interference tests were completed, the construction of the cement foundation could begin, followed by the assembly of the mechanism. The assembly process began with the installation of the support base and the rotation shaft of the azimuth rotation mechanism.

Following this, the structure above the support base was added, completing the assembly of the azimuth rotation mechanism. Figure 4(a) shows the pre-assembly of the elevation rotation

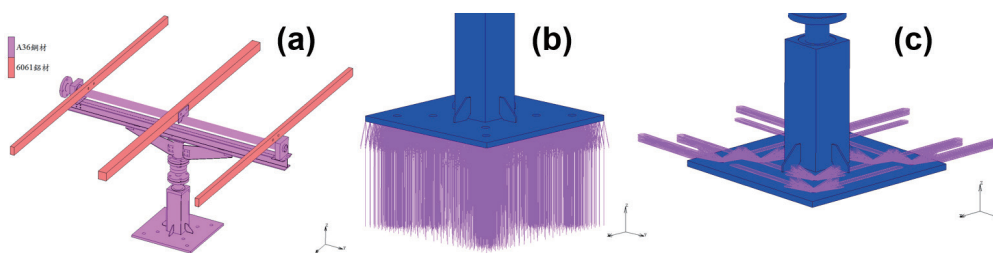


Fig. 3. (Color online) (a) Material setup, (b) boundary condition 1, and (c) boundary condition 2.



Fig. 4. (Color online) Pre-assemblies of (a) elevation rotation mechanism and (b) solar panel truss.

mechanism, where components such as the H-beam, bearing housing, and rotation shaft had already been installed. After the pre-assembly of the elevation rotation mechanism was complete, the solar panel truss was assembled, followed by the solar panel assembly test. As shown in Fig. 4(b), two solar panels had been mounted on the structure. This careful and systematic assembly process was essential to ensure that the system operated smoothly and efficiently in its final form. By performing these preliminary assembling and testing steps, potential issues could be identified and corrected before the final installation, saving both time and resources. This iterative process of pre-assembly and testing reflected a thorough approach to engineering design and manufacturing, ensuring the reliability and functionality of the final system.

The base of the tracking system was constructed using cement as the foundation. Once the cement had fully cured, the assembly process was started. During the assembly, the mechanism's base plate was first leveled using eight nuts to ensure proper alignment. Then, the support base and rotation shaft of the azimuth rotation mechanism were assembled. This step required careful alignment of the thrust bearing on the base plate with the ball bearings on the azimuth rotation shaft, ensuring perfect concentricity. After aligning the mechanism's base, the assembly could continue only after the cement was fully set. Next, the middle and upper shafts of the azimuth rotation mechanism were assembled. Once this part was assembled, the level of the azimuth rotation mechanism was checked, mainly by using a spirit level to ensure the bubble stays within the designated range, indicating proper leveling. Following this, the structures of the elevation rotation mechanism, as shown in Fig. 5(a), and drive mechanism, as shown in Fig. 5(b), were assembled. Finally, the solar panel truss and four solar panels were sequentially installed. The fully assembled mechanism is shown in Fig. 5(c). This meticulous assembly process ensured that each component was precisely aligned and tested for correct functionality before the final installation. By ensuring proper leveling and alignment at every step, the system's stability and performance were optimized, making it ready for reliable operation.

In the original design, the azimuth motor mount's axis center was idealized when modeled in SolidWorks, assuming all conditions were perfect. If the motor is simply fixed to the shaft with a key, without axial support, the axis will sag owing to gravity, causing the gears in the azimuth drive mechanism to fail to mesh properly. To solve this issue, the motor mount was raised by 22.5 mm using small tubes cut from scrap material, allowing the gears to engage and function correctly. The original design for the elevation motor mount used four welded plates, supported



Fig. 5. (Color online) (a) Assembly of rotation structure, (b) assembly of drive mechanism, and (c) completed assembly of tracking system mechanism.

by reinforcing ribs. However, testing revealed slight deformation of the motor mount at certain angles, indicating structural instability. This deformation was attributed to the cantilever beam design, which prevents effective force transmission to the ground, resulting in torsion of the structure. Upon disassembling the DC motor, it was found that the centers of the active and passive shafts were not aligned along the same vertical axis, which was another cause of deformation. To address this, the motor mount design was changed from an “M” shape to a “square” shape, and additional reinforcement was added to both sides of the H-beam to correct the alignment of the axes.

Furthermore, the passive gear’s axis in the elevation drive mechanism was misaligned with the rotation axis of the elevation mechanism itself. This misalignment was likely due to the gap between the flange and the hole or the deformation of the shaft during flange welding, which caused the shaft to tilt during operation. The solution involved adding shims between the screw holes in the two flanges to correct the concentricity of the shafts. The structural design considerations for mechanical assemblies are crucial in ensuring that the components function as intended. In this case, idealizing the conditions in SolidWorks can be helpful for initial design but can lead to problems when real-world forces such as gravity and torque act on the system. The cantilever beam structure, while effective for some applications, is prone to deformation when subjected to significant loads without proper support or force transfer to the ground. Additionally, aligning rotating shafts is a critical step in mechanical design to prevent excessive wear, vibration, and mechanical failure. Misalignment, even at a small scale, can lead to long-term operational inefficiencies and damage to components.

The use of shims to correct misalignment is a straightforward and effective solution, but it highlights the importance of precision in both design and manufacturing to ensure that all parts fit and function as intended. The operational testing conducted after the assembly of the mechanism is a crucial stage in validating the design concepts and actual performance. From a theoretical perspective, these tests not only confirm the motion range of the mechanism but also reveal the manifestation of mechanical principles in real-world applications. The azimuth rotation mechanism demonstrates a full 0-to-360-degree rotational capability, reflecting the complete release of axial degrees of freedom in the design. In mechanism theory, such designs typically employ precise rotary bearing systems combined with appropriate drive mechanisms, enabling unrestricted rotation along the vertical axis. From a dynamics standpoint, achieving

this full rotational capability requires overcoming frictional and inertial torques. The successful test results indicate that the power configuration and gear ratio selection in the drive system were optimized to achieve the desired performance.

The elevation rotation mechanism, according to test results, operates within a ± 52 -degree range. The design of this specific angular range deeply embodies the balance between kinematics and statics in mechanical principles. Theoretically, the elevation adjustment mechanism must strike a balance between motion freedom and structural stability. The ± 52 -degree limitation may stem from intrinsic constraints in the mechanism's geometry, such as the ratio of link lengths to pivot point locations. Additionally, this angular range must account for torque balance under load conditions, especially at the extreme positions where the drive components must provide enough torque to overcome gravity-induced imbalances. The limit position tests shown in Fig. 6 confirm the mechanism's stability at both the maximum elevation (52°) in Fig. 6(a) and the minimum elevation (-52°) in Fig. 6(b). From a mechanical dynamics perspective, limit positions are often regions where mechanical stress concentrates, and the success of these tests demonstrates that material strength and structural rigidity were properly considered in the design. The reliable operation of the mechanism at these extreme positions also confirms that adequate safety margins were accounted for, ensuring safe operation in practical applications.

The intermediate test positions, including -26° , 0° , and 26° , as shown in Figs. 7(a)–7(c), reflect a systematic evaluation of the mechanism's nonlinear characteristics. Theoretically, the mechanism may exhibit varying stiffness, damping properties, and motion precision at different positions. By setting equidistant test points, a comprehensive assessment of the mechanism's performance consistency across its entire motion range was possible. Particularly, the 0-degree

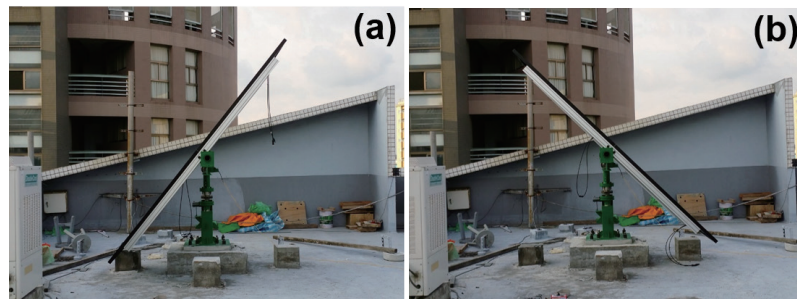


Fig. 6. (Color online) Tilt mechanism: (a) maximum tilt angle of 52° and (b) minimum tilt angle of -52° .



Fig. 7. (Color online) Automatic tracking and rotating mechanism: (a) mechanism tilt angle of 26° , (b) mechanism tilt angle of 0° , and (c) mechanism tilt angle of -26° .

position often represents the system's neutral or balanced point, and its performance at this position has a decisive impact on the overall system's stability. From a broader perspective in mechanism theory, the design of this mechanism may employ a composite kinematic principle, integrating the adjustment functions of both azimuth and elevation. This design needs to account for the coupling effects between the two degrees of freedom, ensuring that the adjustment of one motion axis does not negatively interfere with the other. The test results indicate that the design successfully implemented a decoupling or compensation mechanism between the motion axes.

4. Conclusions

In this study, we presented the design and fabrication of a dual-axis solar tracking system, which, after integrating the design and analysis results, was compared with commercially available tracking systems. The simulation of finite element analysis software was used to conduct various tests, simulations, and analyses, demonstrating that the designed structure offers superior safety and reliability. Finite element simulation results showed that the system could withstand gusts of up to level 17 and endure seismic forces equivalent to a magnitude 5 earthquake. The comparison revealed that the system designed in this research offered several advantages, including low cost, a simple structural design, ease of transport, and quick assembly. The design and manufacturing process drew inspiration from various domestic and international single- and dual-axis solar tracking systems. Through multiple iterations of prototype designs, continuous 3D modeling improvements, and discussions, the final design and fabrication of the dual-axis tracking mechanism were completed. A key feature of the design was its compatibility with commonly available standard components, which reduced the need for custom-made parts, thus achieving the goal of cost control. Additionally, the entire structure could be disassembled, making the system easy to transport. The assembly process was straightforward, requiring only a few workers to set up the system.

Acknowledgments

This research was supported by projects under Nos. NSTC 113-2622-E-390-001 and NSTC 113-2221-E-390-011.

References

- 1 A. George, M. Gibi, A. S. Jacob, M. Diya, and M. Kavya Suresh: 2024 IEEE Inter. Students' Conf. Electrical, Electronics and Computer Science (SCEECS, 2024) pp. 1–5.
- 2 Dual Axis Solar Tracker Systems: Everything To Know About: <https://www.ecosmartinc.com/dual-axis-solar-tracker/> (accessed July 2023).
- 3 H. A. Kazem, M. T. Chaichan, A. H. A. H. Al-Waeli, and K. Sopian: Energy Sources Part A **46** (2024) 15331.
- 4 P. Roth, A. Georgiev, and H. Boudinov: Renew. Energ. **29** (2004) 393.
- 5 W. Batayneh, A. Owais, and M. Nairoukh: Autom. Constr. **29** (2013) 100.
- 6 R. Shaw, S. Das, and S. Kumar: Dual-Axis Solar Tracking System in Advances in Clean Energy Technologies, P. V. Baredar, S. Tangellapalli, and C. S. Solanki Eds. (Springer, Singapore, 2021).
- 7 M. M. Aji, B. G. Gamiya, A. T. Olomowewe, F. A. Ohikere, S. S. Umar, and S. Thomas: 2021 1st Inter. Conf. Multidisciplinary Engineering and Applied Science (ICMEAS, 2021) pp. 1–4.